Validation of use of the miniPCR thermocycler for Ebola and Zika virus detection

Everardo González-González[1,2], Jackelin Lizeth Mendoza-Ramos[1,2], Sara Cristina Pedroza[1,3], Aimé Alexandra Cuellar-Monterrubio[1,3], Alan Roberto Márquez-Ipiña[1,2], Daniel Lira-Serhan[3], Grissel Trujillo-de Santiago[1,3]*, Mario Moisés Alvarez[1,2]*

1 Centro de Biotecnología-FEMSA, Tecnologico de Monterrey, CP, Monterrey, Nuevo León, México,
2 Departamento de Bioingeniería, Tecnologico de Monterrey, CP, Monterrey, Nuevo León, México,
3 Departamento de Ingeniería Mecátrónica y Eléctrica, Tecnologico de Monterrey, CP, Monterrey, Nuevo León, México

* grissel@tec.mx (GTdS); mario.alvarez@tec.mx (MMA)

Abstract

The development of point-of-care (POC) diagnostic systems has received well-deserved attention in recent years in the scientific literature, and many experimental systems show great promise in real settings. However, in the case of an epidemic emergency (or a natural disaster), the first line of response should be based on commercially available and validated resources. Here, we compare the performance and ease of use of the miniPCR, a recently commercially available compact and portable PCR device, and a conventional thermocycler for the diagnostics of viral nucleic acids. We used both thermocyclers to detect and amplify Ebola and Zika DNA sequences of different lengths (in the range of 91 to 300 nucleotides) at different concentrations (in the range of ~50 to 4.0×10^8 DNA copies). Our results suggest that the performance of both thermocyclers is quite similar. Moreover, the portability, ease of use, and reproducibility of the miniPCR makes it a reliable alternative for point-of-care nucleic acid detection and amplification.

Introduction

The development of cost-efficient diagnostic point of care (POC) systems for the opportune diagnosis of infectious diseases is a research niche of high relevance [1,2]. The recent pandemic/epidemic episodes associated with viral diseases (e.g., influenza epi-centered in México in 2009 [3,4], Ebola in West Africa in 2013–2015 [5–7], and Zika in Latin America and Southeast Asia in 2016 [8–10]) are tangible and cruel reminders of the need for portable, low-cost, and easy-to-use diagnostic systems that can effectively address epidemic episodes in remote or underprivileged areas [5,9,11,12].

Many methodologies have been proposed to deliver cost/effective diagnosis (i.e., those based on immunoassays or specific gene hybridization [7,13–16]); however, nucleic acid amplification continues to be the gold standard for the detection of viral diseases in early stages [9,11,17–19]. Among these, the polymerase chain reaction (PCR) is the most established method for molecular diagnostics [10,20]. However, bringing the benefits of PCR to remote or

unprivileged areas has been challenging due to the need for centralized laboratory settings to accomplish traditional PCR testing [21–23], coupled with the still inherently high cost of traditional PCR equipment and reagents [24]. To resolve this drawback, multiple studies have proposed and validated the use of compact PCR-based methods and devices for POC settings [22,25,26].

The first wave of miniaturized PCR machines has only recently become commercially available [27]. The miniPCR from Amplyus (MA, USA) is one of the first highly compact PCR units on the international market [28]. The first miniPCR units reached the marketplace in 2015, with an approximate cost of $600 USD (versus $3000 USD for a conventional PCR thermocycler) [27]. Thus far, only a few papers have been published that directly relate to the validation of use of the miniPCR system as a diagnostic tool[29–33]. For example, Guevara et al. demonstrated its use on the study of wild populations of lemurs in the field [29]. Similarly, Pomerantz et al. demonstrated the combined used of miniPCR and minIon sequencer (a miniaturized sequencer) for the rapid identification of species in the Ecuadorian rainforest [30] (i.e., less than 24 hours after data collection). Boguraev et al. successfully amplified zebrafish DNA in a remarkably non-conventional setting—aboard the International Space Station—and they were able to amplify bisulfite-treated DNA to determine epigenetic variations. They found that methylation-specific primers differentially amplified bisulfite-treated DNA just as would be expected under standard laboratory conditions on Earth [31]. Recently, Zaky et al. used the miniPCR system for the detection of Brugia parasites in mosquitos [33]. The commercial availability, low price (as compared to conventional thermocyclers), portability, and user friendliness make the miniPCR an attractive and tangible solution that effectively brings PCR analysis to the POC.

In the case of evaluating the spread of an infectious disease, the deployment of any diagnostic effort has to rely first on commercially available equipment [34]. Consequently, a comparison of current commercially available compact PCR platforms is of paramount importance. Here, we compare the sensitivity, reproducibility, and convenience of use of the miniPCR (www.minipcr.com) versus a conventional and commercially available PCR thermocycler for the detection and amplification of synthetic samples of Ebola virus and Zika (ZIKV) virus. The *Zaire ebolavirus* (EBOV)[35] and ZIKV have caused the two most recent widespread international epidemic emergencies. From 2014 to 2016, West Africa was the site of the most important Ebola epidemic documented so far; more than 20,000 persons were infected and more than 11,000 died of this disease. From 2015 to 2016, a ZIKV epidemic episode affecting Las Americas reached alarming proportions. The association of ZIKV with recent cases of microcephalic births has increased the concern about establishing systems for early diagnosis [9,36].

Materials and methods

Equipment specifications

We ran equivalent sets of amplification experiments in a commercial standard thermocycler (MaxyGene from Axygen, CA, USA) and a miniPCR from Amplyus (MA, USA). The MaxyGene unit can run 96 amplifications simultaneously, has dimensions of 25×25×25 cm, and a weight of 3.5 kg. This unit requires 120V (AC) and 3.5 A to operate. The miniPCR can run 8 amplifications in parallel, has dimensions of 20×5×15 cm, and a weight of 0.7 kg. This unit requires 120V (AC) and 3.5 A to operate.

A commercial power supply (PowerPac from Bio-Rad, CA, USA) was used to operate the electrophoresis unit in which the agarose gels were run to reveal the amplification products obtained by both the MaxyGene and the miniPCR thermocyclers. A Bio-Rad ChemiDoc XRS imaging system was used for end-point PCR detection. Alternatively, the miniPCR unit has its
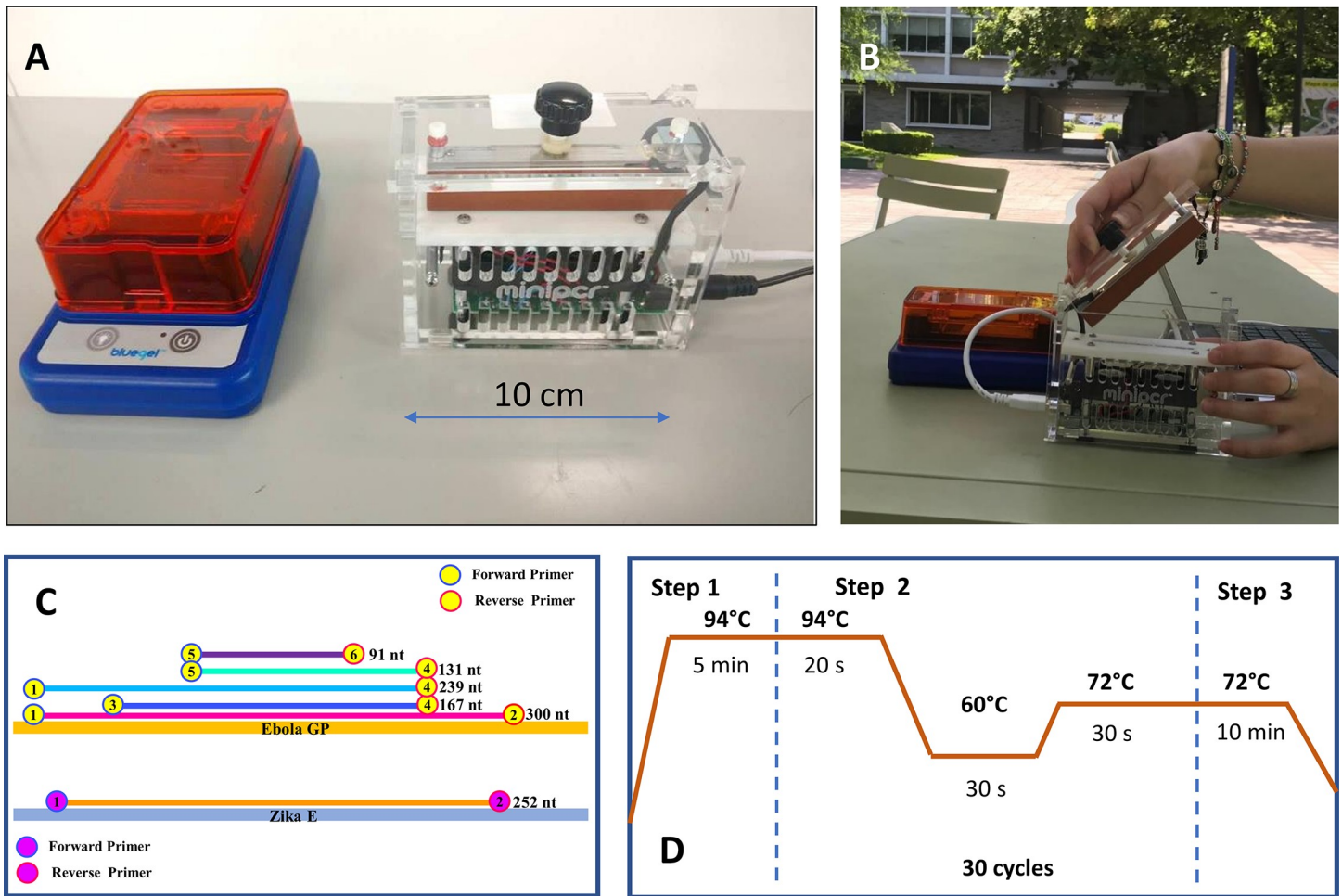
Fig 1. A) The miniPCR thermocycler and blueGel electrophoretic chamber. B) Outdoor use of the miniPCR device. Portability, ease of use, and low toxicity of the reagents allow genetic material amplification outside the laboratory. C) Amplicons of various lengths can be obtained using different sets of primers targeting a sequence encoding the Ebola virus GP protein. D) Temperature cycling scheme used in our PCR protocol.

own blueGel electrophoresis unit (Fig 1A and 1B), powered by 120 AC volts, and photo-documentation can be done using a smartphone camera.

Samples and sample preparation

We used synthetic samples containing EBOV and ZIKV nucleic acids in our validation experiments. We prepared the EBOV samples by cloning a genetic sequence (Table 1) encoding the production of the EBOV GP capsid protein in an *Escherichia* coli strain (TOP10). Similarly, we cloned a genetic sequence encoding the production of the ZIKV E capsid protein in an *E. coli* strain (TOP10) to produce ZIKV nucleic acid material (Table 1). The EBOV sequence was designed based on the consensus of GP sequences of the *Zaire ebolavirus* documented in GenBank from 1976–2014 (S1 Fig). The ZIKV sequence was designed by considering the consensus of the E gene sequences of the ZIKV strains documented globally in GenBank from 2013–2016 (S2 Fig).

The engineered bacterial strains were cultured overnight in LB-media (250ml) at 37˚C in Erlenmeyer flasks under orbital agitation at 200 RPM. After 12 hours of culture, the bacteria

were harvested by centrifugation and then lysed using a continuous homogenizer. Synthetic viral DNA was purified from the bacterial samples using the PureYield Plasmid Maxiprep System (Promega, WI, USA). Samples containing different concentrations of synthetic nucleic acids of EBOV and ZIKV were prepared by successive dilutions from stocks containing 400 ng/L of viral nucleic acids.

Amplification mix

We used REDTaq Ready Mix from Sigma-Aldrich (USA), and followed the recommended protocol: 5 μL Readymix, 1 μL of forward primer, 1 μL of reverse primer (for a final concentration of 0.5 μM), 1 μL of DNA template (3ng to 5 x 10^{-7} ng; ~ 66 to 3.9 x 10^8 DNA copies), and nuclease free water to final volume of reaction 10 μL.

Primers used

Three different sets of primers were used to target a region of the EBOV GP sequence. One set of primers was used to target a region that encodes the ZIKV E protein (Fig 1C). Sequences of all these primers and their corresponding amplicons are presented in Tables 2 and 3.

Amplification protocols

For all PCR experiments, we used the same three-stage protocol (see Fig 1D) consisting of a denaturation stage at 94°C for 5 min, followed by 30 cycles of 94°C for 20s, 60°C for 30s, and 72°C for 30s, and then a final stage at 72°C for 10 min, with a total duration of 76 and 80 minutes in the MaxyGene and the miniPCR thermocyclers, respectively.

Documentation of PCR products

We analyzed 10μL of each PCR product using 1% agarose electrophoresis in TAE (Tris-Acetic Acid-EDTA) buffer (Sigma-Aldrich, MO, USA). Gels were dyed with GelGreen (CA, USA) using a 1:10,000 dilution and a current of 110 V supplied by a Bio-Rad PowerPac HC power supply (Bio-Rad, CA, USA) for 50 minutes. We used the Quick-Load Purple 2-Log DNA Ladder (NEB, MA, USA) as molecular a molecular weight marker. We analyzed the gels by UV transillumination using a Bio-Rad ChemiDoc XRS imaging system.

In addition, in some of our experiments, we used the blueGel unit, a portable electrophoresis unit sold by MiniPCR from Amplyus (MA, USA). This is a compact electrophoresis unit (23 × 10 × 7 cm) that weighs 350 g. In these experiments, we analyzed 10μL PCR product using 1% agarose electrophoresis tris-borate-EDTA buffer (TBE). Gels were dyed with Gel-Green (CA, USA) using a 1:10,000 dilution, and a current of 48V was supplied by the bluegel built-in power supply (AC 100-240V, 50-60hz).

Additional quantification strategies for PCR products

We evaluated the total amount of amplified nucleic acids (as quantified by absorbance analysis at 260 nm) and their purity (as quantified by the 260/280 ratio) using a Nanodrop 1000 spectrophotometer (Thermo Fisher Scientific, MA, USA). In these experiments, 10μL of PCR product was purified using the Wizard SV Gel and PCR Clean-Up kits (Promega, WI, USA), and the purified DNA (average yield of 41.5ng/μL) was re-suspended and dissolved in 50 μL of nuclease-free water.

In an additional set of experiments, the amount of amplified DNA was determined by staining with Brilliant III Ultra-Fast SYBR Green QPCR Master Mix (Agilent Technologies CA, USA). We used 0.5 ng of synthetic EBOV or ZIKV as a DNA template, 2 μl of forward primer

Table 1. Nucleotide sequences used to engineer bacterial strains to produce Ebola virus (EBOV) and Zika virus (ZIKV) nucleic acids.

Target gene	Nucleotide sequence
Ebola GP$^\alpha$ protein (capsid)	**EBOV-GP:** ATGTCTACCGAGTCTATGATTAGGGACGTGGAACTGGCTGAGGAGGCACTGCCCAAAAAAACCGGCGGACCA CAGGGCTCTAGGAGATGTCTGTTTCTGTCTCTGTTCTCTTTTCTCATCGTGGCTGGCGCTACAACACTCTTCT GTCTGCTCCATTTCGGCGTGATTGGACCACAGCGAGAGGAATTTCCCCGGGATCTGTCACTCATTTCACCAC TGGCCACAGGCTGTCCGATCTTCATCTCGGACTCCATCCGACAAACCTGTCGCCCATGTCGTCGCCAACCC ACAGGCCGAGGGCCAGCTCCAGTGGCTCAATAGGAGGGCAAACGCTCTGCTCGCCAATGGCGTGGAACTC CGGGATAACCAGCTCGTCGTGCCTAGTGAGGGACTGTACCTCATCTACTCCCAGGTGCTGTTTAAGGGCC AGGGATGTCCTTCTACACATGTGCTGCTCACACACACAATTTCACGGATCGCCGTGTCTTACCAGACTAA AGTCAATCTGCTCTCTGCCATCAAATCCCCATGTCAGCGGGAAACACCTGAGGGCGCTGAGGCTAAACC TTGGTACGAACCCATCTACCTCGGAGGCGTGTTCCAGCTGGAGAAGGGCGATAGACTGAGTGCTGAG ATCAATCGACCCGACTACCTCGACTTTGCCGAATCTGGCCAGGTCTACTTTGGCATCATTGCTCTGG GCCTCGAGGGCCGAGCTCATGGCGCACCTAGGCCTTTGAATTCCTCTACCGAGTCTATGATTAGGGA CGTGGAACTGGCTGAGGAGGCACTGCCCAAAAAAACCGGCGGACCACAGGGCTCTAGGAGATGTCTGT TTCTGTCTCTGTTCTCTTTTCTCATCGTGGCTGGCGCTACAACACTCTTCTGTCTGCTCCATTTCGGCGT GATTGGACCACAGCGAGAGGAATTTCCCCGGGATCTGTCACTCATTTCACCACTGGCCACAGGCTGTCC GATCTTCATCTCGGACTCCATCCGACAAACCTGTCGCCCATGTCGTCGCCAACCCACAGGCCGAGGG CCAGCTCCAGTGGCTCAATAGGAGGGCAAACGCTCTGCTCGCCAATGGCGTGGAACTCCGGGAT AACCAGCTCGTCGTGCCTAGTGAGGGACTGTACCTCATCTACTCCCAGGTGCTGTTTAAGGGCC AGGGATGTCCTTCTACACATGTGCTGCTCACACACACAATTTCACGGATCGCCGTGTCTTACCAGACTAAAG TCAATCTGCTCTCTGCCATCAAATCCCCATGTCAGCGGGAAACACCTGAGGGCGCTGAGGCTAAACC TTGGTACGAACCCATCTACCTCGGAGGCGTGTTCCAGCTGGAGAAGGGCGATAGACTGAGTGCTGA GATCAATCGACCCGACTACCTCGACTTTGCCGAATCTGGCCAGGTCTACTTTGGCATCATTGCT CTGGGCCTCGAGGGCCGAGCTCATGGCGCACCTAGGCCTTTGAATTCCTCTACCGAGTCTATGATTAGGGAC GTGGAACTGGCTGAGGAGGCACTGCCCAAAAAAACCGGCGGACCACAGGGCTCTAGGAGATGTCTGTT TCTGTCTCTGTTCTCTTTTCTCATCGTGGCTGGCGCTACAACACTCTTCTGTCTGCTCCATTTCGGCG TGATTGGACCACAGCGAGAGGAATTTCCCCGGGATCTGTCACTCATTTCACCACTGGCCACAGGCTGT CCGATCTTCATCTCGGACTCCATCCGACAAACCTGTCGCCCATGTCGTCGCCAACCCACAGGCCGAG GGCCAGCTCCAGTGGCTCAATAGGAGGGCAAACGCTCTGCTCGCCAATGGCGTGGAACTCCGGGAT AACCAGCTCGTCGTGCCTAGTGAGGGACTGTACCTCATCTACTCCCAGGTGCTGTTTAAGGGCCAG GGATGTCCTTCTACACATGTGCTGCTCACACACACAATTTCACGGATCGCCGTGTCTTACCAGACT AAAGTCAATCTGCTCTCTGCCATCAAATCCCCATGTCAGCGGGAAACACCTGAGGGCGCTGAGGC TAAACCTTGGTACGAACCCATCTACCTCGGAGGCGTGTTCCAGCTGGAGAAGGGCGATAGACTGA GTGCTGAGATCAATCGACCCGACTACCTCGACTTTGCCGAATCTGGCCAGGTCTACTTTGGCATCA TTGCTCTGGGCCTCGAGGGCCGAGCTCATGGCGCACCTAGGCCTTTGA
Zika E$^\beta$ protein (capside)	**ZIKV-E:** ATGATCAGGTGCATAGGAGTCAGCAATAGGGACTTTGTGGAAGGTATGTCAGGTGGGACTTGGG TTGATGTTGTCTTGGAACATGGAGGTTGTGTCACCGTAATGGCACAGGACAAACCGACTGTCGACATAGAGCT GGTTACAACAACAGTCAGCAACATGGCGGAGGTAAGATCCTACTGCTATGAGGCATCAATATCAGACAT GGCTTCGGACAGCCGCTGCCCAACACAAGGTGAAGCCTACCTTGACAAGCAATCAGACACTCAATATGTCTG CAAAAGAACGTTAGTGGACAGAGGCTGGGGAAATGGATGTGGACTTTTTGGCAAAGGGAGCCTG GTGACATGCGCTAAGTTTGCATGCTCCAAGAAAATGACCGGGAAGAGCATCCAGCCAGAGAATC TGGAGTACCGGATAATGCTGTCAGTTCATGGCTCCCAGCACAGTGGGATGATCGTTAATGACA CAGGACATGAAACTGATGAGAATAGAGCGAAGGTTGAGATAACGCCCAATTCACCAAGAGCC GAAGCCACCCTGGGGGGTTTTGGAAGCCTAGGACTTGATTGTGAACCGAGGACAGGCCTT GACTTTTCAGATTTGTATTACTTGACTATGAATAACAAGCACTGGTTGGTTCACAAGGAGTG GTTCCACGACATTCCATTACCTTGGCACGCTGGGGCAGACACCGGAACTCCACACTGGAACA ACAAAGAAGCACTGGTAGAGTTCAAGGACGCACATGCCAAAAGGCAAACTGTCGTGGTTCTA GGGAGTCAAGAAGGAGCAGTTCACACGGCCCTTGCTGGAGCTCTGGAGGCTGAGATGGATGG TGCAAAGGGAAGGCTGTCCTCTGGCCACTTGAAATGTCGCCTGAAAATGGATAAACTTAGAT TGAAGGGCGTGTCATACTCCTTGTGTACCGCAGCGTTCACATTCACCAAGATCCCGGCTGAA ACACTGCACGGGACAGTCACAGTGGAGGTACAGTACGCAGGGACAGATGGACCTTGCAAGGT TCCAGCTCAGATGGCGGTGGACATGCAAACTCTGACCCCAGTTGGGAGGTTGATAACCGCTA ACCCCGTAATCACTGAAAGCACTGAGAACTCTAAGATGATGCTGGAACTTGATCCACCATTT GGGGACTCTTACATTGTCATAGGAGTCGGGGAGAAGAAGATCACCCACCACTGGCACAGGA GTGGCAGCACCATTGGAAAAGCATTTGAAGCCACTGTGAGAGGTGCCAAGAGAATGGCAGTC TTGGGAGACACAGCCTGGGACTTTGGATCAGTTGGAGGCGCTCTCAACTCATTGGGCAAGGG CATCCATCAAATTTTTGGAGCAGCTTTCAAATCATTGTTTGGAGGAATGTCCTGGTTCTCACAA ATTCTCATTGGAACGTTGCTGATGTGGTTGGGTCTGAACACAAAGAATGGATCTATTTCCCTTAT GTGCTTGGCCTTAGGGGGAGTGTTGATCTTCTTATCCACAGCCGTCTCTGCTCATCATCATCATCA TCATTGA

$^\alpha$Most abundant EBOV capsid protein; molecular weight = 74 kDa
$^\beta$Most antigenic ZIKV protein; molecular weight = 54 kDa.

https://doi.org/10.1371/journal.pone.0215642.t001

solution, 2 µl of reverse primer solution, 10 µl of 2× SYBR Green QPCR master mix, and nuclease-free PCR-grade water to adjust the final volume to 20 µl. After the PCR reaction was

Table 2. Primer sequences used in PCR amplification experiments and their corresponding amplicons.

Target gene	Primers sequences
Ebola GP gene (capsid)	EBOV1: ACACTACTGGGAAGCTGATCTGGAAAGTCA EBOV2: AGGTGGTGAGGTGCGACACGGCCGCTTCGC EBOV3: AAACCAAGAAGAACCTGACCAGAAAGATCC EBOV4: GCTGTTTTCGCTAGCCATAATCTTATGATC EBOV5: AGGAGCTGTCCTTCACCGTGGTGTCAAATG EBOV6: GTGTTAGTACCCGGGTCGGATGAGGTGCGC
Zika E gene (capsid)	ZIKV1: AGCCGAAGCCACCCTGGGGGGTTTTGGAAG ZIKV2: CCTAGAACCACGACAGTTTGCCTTTTGGCA

https://doi.org/10.1371/journal.pone.0215642.t002

completed (3 minutes at 95°C; 40 cycles of 5 seconds at 95°C, and 12 seconds at 60°C), the amplification product was transferred to a 7500 Fast Real-Time PCR System (Thermo Fisher Scientific, MA, USA). The amount of amplification product was determined by fluorescence measurements using a SYBR Green filter. For this purpose, 10 cycles of 10 seconds at 21°C were programmed in the Real-Time PCR System. The reading from the fourth cycle was used for statistical analysis.

Results and discussion

Previous epidemic episodes (for example, those related to EBOV in West Africa in 2014–2016) have proven that an actual emergency does not provide the required timeframe for testing new strategies. This is true for new therapies as well as for diagnosis. In the case of epidemic emergencies (or natural disasters), the first line of response must be based on commercially available and validated resources. Here, we compare the performance of a commercially available portable PCR unit (aimed at several markets, including POC applications) versus that of a conventional, regular-sized PCR thermocycler. The comparison was made in terms of the ability of both units to identify and amplify different synthetically designed genetic sequences of

Table 3. Amplicon sequences generated (and their corresponding length) by each of the primer pairs used in the PCR amplification experiments (see also Fig 1C).

Primers	Amplicon sequence	Amplicon Length (nt)
EBOV1–EBOV2	ACACTACTGGGAAGCTGATCTGGAAAGTCAACCCGGAGATCGACACTACGATCGGAGAGTGGGCCTTTTGGGAAAC CAAGAAGAACCTGACCAGAAAGATCCGGTCCGAGGAGCTGTCCTTCACCGTGGTGTCAAATGGCGCCAAGAACATC TCGGGACAGTCTCCCGCGCGCACCTCATCCGACCCGGGTACTAACACCACTACCGAGGATCATAAGATTATGGCTAG CGAAAACAGCTCGGCCATGGTGCAAGTCCACAGCCAGGGACGCGAAGCGGCCGTGTCGCACCTCACCACCT	300
EBOV3–EBOV4	AAACCAAGAAGAACCTGACCAGAAAGATCCGGTCCGAGGAGCTGTCCTTCACCGTGGTGTCAAATGGCGCCAA GAACATCTCGGGACAGTCTCCCGCGCGCACCTCATCCGACCCGGGTACTAACACCACTACCGAGGATCATA AGATTATGGCTAGCGAAAACAGC	167
EBOV5–EBOV6	AGGAGCTGTCCTTCACCGTGGTGTCAAATGGCGCCAAGAACATCTCGGGACAGTCTCCCGCGCGCACCT CATCCGACCCGGGTACTAACAC	91
EBOV1–EBOV4	ACACTACTGGGAAGCTGATCTGGAAAGTCAACCCGGAGATCGACACTACGATCGGAGAGTGGGCCTTTTGGGAA ACCAAGAAGAACCTGACCAGAAAGATCCGGTCCGAGGAGCTGTCCTTCACCGTGGTGTCAAATGGCGCC AAGAACATCTCGGGACAGTCTCCCGCGCGCACCTCATCCGACCCGGGTACTAACACCACTACCGAGGAT CATAAGATTATGGCTAGCGAAAACAGC	239
EBOV5–EBOV4	AGGAGCTGTCCTTCACCGTGGTGTCAAATGGCGCCAAGAACATCTCGGGACAGTCTCCCGCGCGCACC TCATCCGACCCGGGTACTAACACCACTACCGAGGATCATAAGATTATGGCTAGCGAAAACAGC	131
ZIKV1–ZIKV2	AGCCGAAGCCACCCTGGGGGGTTTTGGAAGCCTAGGACTTGATTGTGAACCGAGGACAGGCCTTGA CTTTTCAGATTTGTATTACTTGACTATGAATAACAAGCACTGGTTGGTTCACAAGGAGTGGTTCCAC GACATTCCATTACCTTGGCACGCTGGGGCAGACACCGGAACTCCACACTGGAACAACAAAGAAGCAC TGGTAGAGTTCAAGGACGCACATGCCAAAAGGCAAACTGTCGTGGTTCTAGG	252

https://doi.org/10.1371/journal.pone.0215642.t003

EVOB and ZIKV under the same set of experimental protocols and using the same materials and reagents (see Materials and Methods).

Engineering of target sequences and primers

For the case of EBOV detection, we designed and synthetized a construct to enable the expression of the EBOV GP protein in *E.coli*. GP, an antigenic glycoprotein abundantly present in the EBOV capsid, has been widely studied in literature [6]. The GP construct was cloned in the TOP10 *E. coli* strain. The culture and harvest of expressing clones of the bacteria allowed the collection of genetic DNA of EBOV without resorting to the use or propagation of the real virus [4]. For the case of ZIKV detection, we used the same strategy for synthetic production of nucleic acid sequences encoding the ZIKV E protein (Table 1). The flavivirus envelope (E) glycoprotein is a structural protein and is responsible for virus entry (attachment, membrane fusion, and virion assembly); it therefore represents a major target for neutralizing antibodies.

Table 2 shows the sets of primers used to target genetic sequences that code for the expression of the EBOV GP protein and the ZIKV E protein. EBOV and ZIKV were selected for this validation study because they were responsible for two of the most recent international epidemic emergencies of viral origin. The EBOV variant Makona was the causal agent of the West Africa Ebola epidemics [37,38], while ZIKV was the causal agent of a recent epidemic event that spanned most of Latin America and a significant portion of the United States in 2016 [5–10].

Effect of amplicon length

We conducted different sets of experiments to compare the performance of the miniPCR and a conventional commercial thermocycler. In a first round of experiments, we used five different sets of primers of different lengths that target different regions within the selected EBOV GP sequence. The lengths and sequences of each of the amplicons generated by each set of primers are presented in Tables 2 and 3. Fig 1C graphically shows the regions of the EBOV GP sequence to which each primer set binds and the length of each of the originated amplicons. These sets of primers generated PCR products of 91, 131, 167, 239, and 300 nucleotides (nt). Fig 2A shows images of a representative agarose gel experiment for the PCR products of different amplification reactions using different primer combinations. Products obtained using the miniPCR and the conventional thermocycler are presented. These results show that the use of primer sets designed to produce PCR products of different lengths has no meaningful effect on the performance of the amplifications. Moreover, we did not observe any substantial differences between the performance of the miniPCR and the conventional thermocycler. In addition, our use of a multiplex PCR strategy did not result in any obvious advantage over the use of conventional PCR; this observation holds for reactions conducted using both the miniPCR and the conventional thermocycler.

Interestingly, the profile of amplification products from the multiplexed reactions differed between the mini-PCR and the conventional thermocycler (Fig 2A). In an ideal multiplex PCR [39], where all targeted sequences are equally accessible to primer pairs and the polymerase, denser (more intense) bands are expected for the higher molecular weight amplification products (more base pairs per amplicon unit) than for the lower molecular weight products. Consistently, the higher molecular weight product of the multiplex reaction appears as a darker band in the miniPCR amplification. However, this is not the case for the conventional PCR results. This finding, which was consistent among experimental repeats, suggests a tighter control of the PCR microenvironmental conditions (i.e., mixing, temperature homogeneity, etc.) within the miniPCR reaction cells.

Fig 2. Comparison of the miniPCR and Maxygen thermocyclers using primer sets that yield different amplicon sizes. (A) Comparative images of agarose gel electrophoresis of DNA coding for EBOV GP protein using miniPCR and Maxygen thermocyclers. Different amplicon sizes obtained using the miniPCR (left section) and Maxygen (right section) thermal cyclers. From left to right: 91 bp (lane 1), 131 bp (lane 2), 167 bp (lane 3), 239 bp (lane 4), and 300 bp (lane 5), multiplex amplification of 91 and 167 bp (lane 6), and a negative control (lane 7). B) Evaluation of the amount of miniPCR-amplified DNA (as measured by Nanodrop Spectrometry at 260 nm), and (C) the purity (absorbance ratio at 260/280 nm) of DNA produced by primer sets that produce amplicons of different sizes. Primers that were aimed to produce amplicons of 91bp produced statistically lower amounts of DNA in miniPCR amplification experiments (p-value < 0.05). All primer sets yielded amplification products with statistically similar purities (p-value >> 0.05). Error bars indicate one standard deviation.

We further evaluated the effect of using primers that yield amplification products of different sizes (namely 91, 167, and 300 bp) in the miniPCR thermocycler. For this purpose, we conducted experiments in which we determined the amount of DNA produced by miniPCR amplifications using NanoDrop spectrophotometry. For this experimental set, we used 0.5 ng of EBOV DNA template. Our results suggest that the total amount of amplification product is statistically lower with the use of primers that flank a region of 91 bp (Fig 2B). This is an expected result; primers aimed at producing shorter amplicons should render less DNA per cycle. However, the purity of the DNA obtained in reactions using all different primer sets is statistically similar (Fig 2C). Moreover, the amount of amplification product is statistically similar for reaction protocols that yield amplicons of 167 and 300 bp (Fig 2B). These results suggest that the use of primers of about 150bp in size for miniPCR amplifications will render similar results, in terms of DNA quantity and quality, as those obtained with larger primers. The total amount and purity of amplification product was statistically similar for multiplex amplification (using primers that yield amplicons of 91 and 167 bp) and single primer amplification (using primers that yield amplicons of 167 or 300bp) (Fig 2B and 2C). This observation is based on final-point PCR results; in a real-time amplification, multiplexing might provide faster results.

Analysis of sensitivity

Next, we conducted a second series of experiments to assess the sensitivity of the PCR reactions conducted in both thermocyclers using primers that generate amplicons of two different sizes. Fig 3A and 3B show the PCR products of amplification reactions conducted using a set of primers that produce amplicons of 91 nt and a 300 bp, respectively. In both cases, different concentrations of EBOV-GP genetic material, in the range of 5×10^{-7} to 3.0 ng/10 μL, were used as reaction template. The amplification proceeds with sufficient quality to allow proper visualization of the amplification product, even at low nucleic acid concentrations. However, we observed differences in the profile of the products of amplification when using primers to flank regions of 91 or 300 nt (compare Fig 3A and 3B). For instance, at low DNA template concentrations, the primers that flank the 91nt region appears to be more effective than those that target the 300nt region. In this set of experiments, we were particularly careful to ensure the integrity of the genetic material used as a template. Evidently, under real conditions, the integrity of larger templates can be more compromised by environmental factors when compared to shorter DNA segments, so targeting shorter nucleic DNA sequences might be advantageous [40,41]. Moreover, in the range of DNA concentrations explored, we did not observe any conclusive difference in performance between the miniPCR and the conventional thermocycler.

In an additional experiment, we challenged the sensitivity of both PCR thermocyclers with a different set of primers. This time, we amplified a ZIKV sequence, aiming to produce an amplicon of 252 base pairs (bp). Different concentrations of ZIKV genetic material, in the range of 5×10^{-7} to 3.0 ng/10 μL, were used as reaction template. Fig 2C presents an agarose gel showing the amplification products of this experiment. As before, we observed a similar performance between thermocyclers. Both the miniPCR and the conventional systems were able to generate a visible band of amplification products across the whole range of DNA dilutions.

Robustness of the miniPCR system

In a final set of experiments, we tested the robustness of the miniPCR system from two different angles. First, we validated the reproducibility of the results generated by the miniPCR between different assay wells. For that purpose, we dispensed the same sample of DNA (EBOV
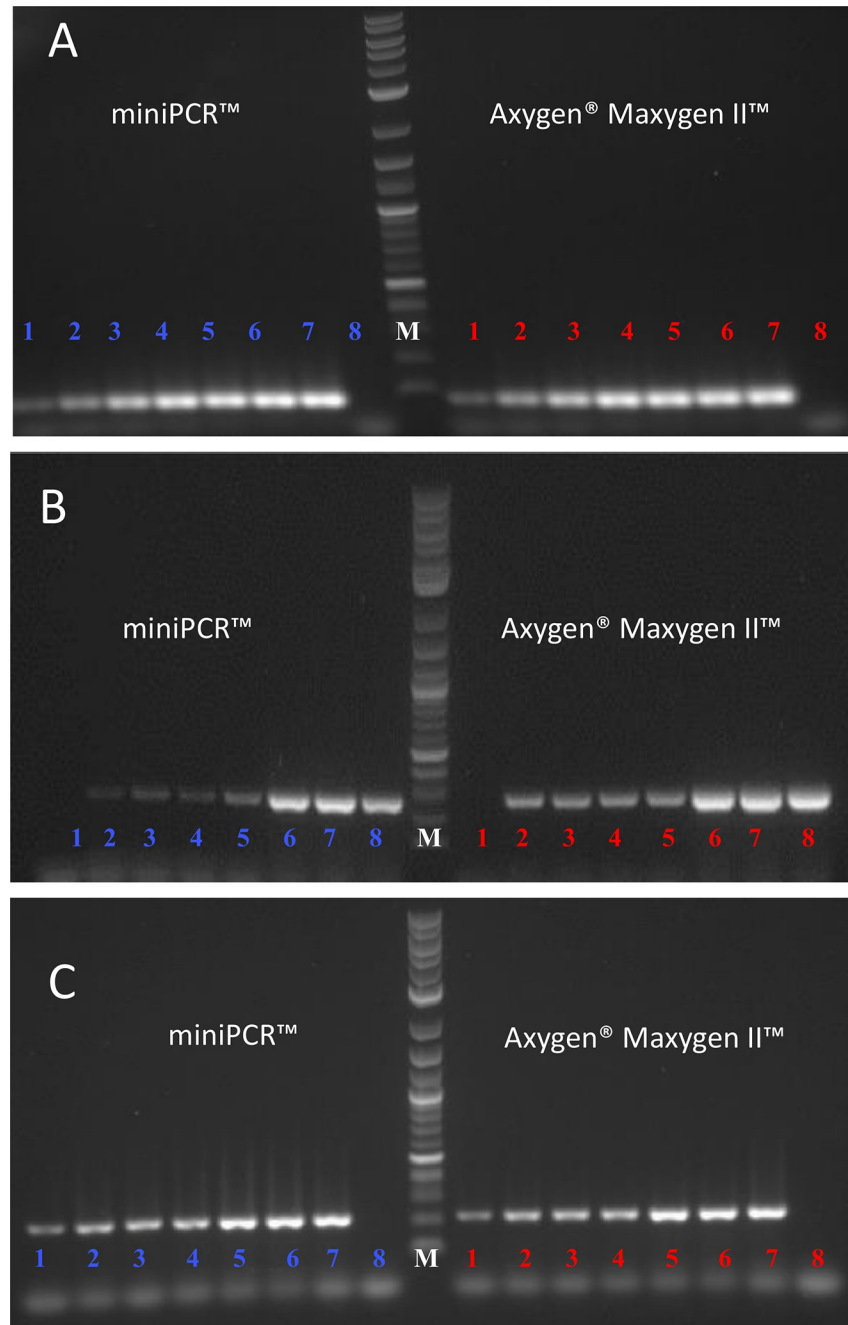
Fig 3. Comparison of sensitivity between the miniPCR and Maxygen thermal cyclers. A) Sensitivity trials using a 91 bp amplicon in miniPCR (left section) and Maxygen (right section) thermal cyclers. The initial template amount was gradually increased from left to right: 66 (lane 1), 6.62×10^2 (lane 2), 6.62×10^4 (lanes 3), 6.62×10^6 (lane 4), 6.62×10^7 (lane 5), 1.30×10^8 (lane 6), and 3.9×10^8 DNA copies (lane 7), and negative control (lane 8). B). Sensitivity trials using a 300bp amplicon in the miniPCR (left section) and Maxygen (right section) thermal cyclers. The initial template amount was gradually increased from left to right: negative control (lane 1), 66 (lane 2), 6.62×10^2 (lane 3), 6.62×10^4 (lanes 4), 6.62×10^6 (lane 5), 6.62×10^7 (lane 6), 1.30×10^8 (lane 7), and 3.9×10^8 DNA copies (lane 8). These results showed no significant differences between devices. (C) Sensitivity trials using a 252bp Zika virus amplicon in the miniPCR (left section) and Maxygen (right section) thermal cyclers. The initial template amount was gradually increased from left to right: 66 (lane 1), 6.62×10^2 (lane 2), 6.62×10^4 (lane 3), 6.62×10^6 (lane 4), 6.62×10^7 (lane 5), 1.30×10^8 (lane 6), and 3.9×10^8 DNA copies (lane 7), and negative control (lane 8).
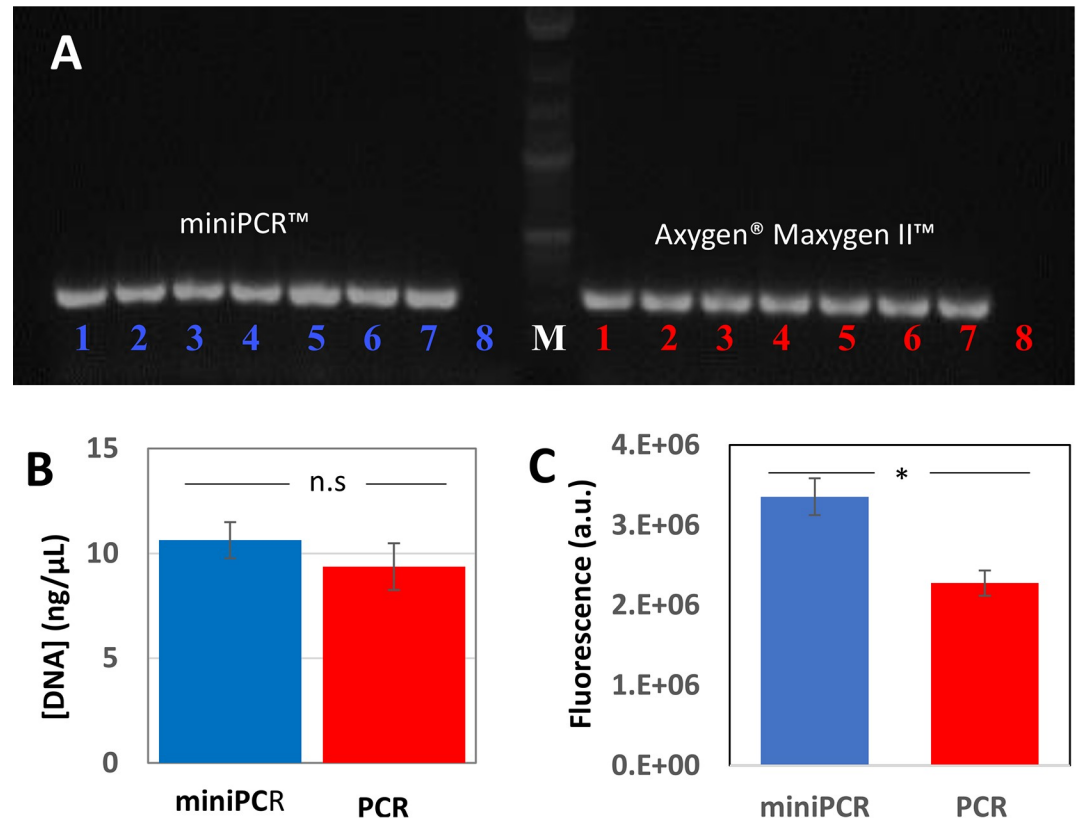
Fig 4. Comparison of the amount of amplification product produced by miniPCR (left section) and Maxygen (right section) thermal cyclers. A) Repeatability test using an initial amount of 0.5ng of a 300bp amplicon corresponding to the Ebola virus GP protein in the miniPCR (left section) and Maxygen (right section) thermal cyclers. Seven repeats (lane 1 to 7) and a negative control (lane 8) are shown. B) Average amount of nucleic acid material recovered from the agarose gels. No significant differences were noted between devices (p-value > 0.05). Error bars indicate one standard deviation. C) Average amount of nucleic acid material recovered, as quantified by SYBR Green qPCR staining and fluorescence measurements in a real time thermocycler. Significant differences were noted between devices (p-value* = 0.043). Error bars indicate one standard deviation.

https://doi.org/10.1371/journal.pone.0215642.g004

genetic material; at 0.5 ng/μL; expected amplicon of 300bp) in seven of the eight amplification wells of the miniPCR thermocycler (one well was left as a negative control). For comparison, the same amplification experiment was performed in eight of the amplification cells of the conventional PCR system, selected at random. Fig 4A shows an agarose gel of the amplification products for eight different wells of both thermocyclers. We did not observe any significant variations in intensity among the wells in any thermocycles. In addition, we quantified the intensities of the bands corresponding to amplification products using band purification and nanodrop quantification. The results revealed small standard deviations for both sets of samples. Both thermocyclers also performed similarly in terms of reproducibility; the average amounts of amplification products were statistically similar for both data sets (α-value = 0.5; Fig 4B).

In an additional set of experiments, we quantified the amount of DNA amplified in different assay wells (in both thermocyclers) using SYBR Green staining followed by fluorescence determination in a RT-PCR apparatus (Fig 4C). The results confirm that both thermocyclers are similar in terms of reproducibility, as both exhibited a variance coefficient of ~0.06.

Interestingly, in these experiments (without purification), the miniPCR thermocycler produced significantly higher amounts of DNA than were obtained with the conventional thermocycler.

In all previously described experiments, the products of amplification from both thermocyclers were primarily detected on agarose gels using conventional electrophoresis techniques conducted with conventional lab equipment. However, as previously mentioned, the miniPCR system is commercialized with its own "blueGel" electrophoretic unit (Fig 5A). In a last set of experiments, we separated the amplification products using the miniPCR electrophoretic unit to assess its practicality and reliability. Fig 5B shows a gel that displays the products of amplification of a typical experiment where EBOV sequences were targeted.

Besides its portability, the blueGel electrophoretic unit has other important advantages: its size allows optimization of reagent usage (agarose gel 15ml, buffer 25ml), the built-in power supply allows visualization of band separation in real time, which can shorten the electrophoretic time by up to 5 minutes; and exposure to ethidium bromide and UV light is completely avoided by the use of GelGreen dye and detection with blue light.

Conclusions

The challenge of POC detection of viral threats is of paramount importance, particularly in underdeveloped regions and in emergency situations (i.e., natural disasters or epidemic outbreaks). In the context of an emergency, time is very limited (as are other resources) to do research or develop new technologies; therefore, the use of commercially available and tested technologies is an obvious first countermeasure. Our research extends the validation of the miniPCR technology to the as yet unexplored topic of detection of Ebola and Zika, and we
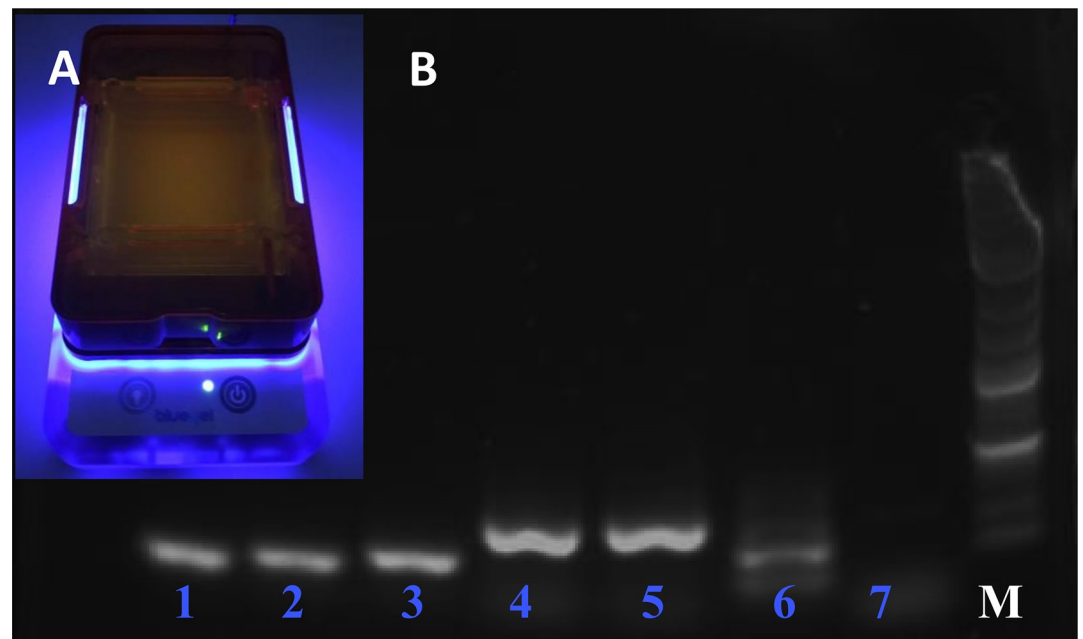
Fig 5. The blueGel electrophoresis chamber: blueGel (A) allows visualization of a 15 ml agarose gel using an integrated blue LED array. B) Agarose gel electrophoresis of Ebola virus amplification products of different sizes using the miniPCR thermocycler and blueGel electrophoretic chamber: 91 bp (lane 1), 131 bp (lane 2), 167 bp (lane 3), 239 bp (lane 4), 300 bp (lane 5), multiplex amplification of 91and 167 bp (lane 6), and negative control (lane 7).

https://doi.org/10.1371/journal.pone.0215642.g005

have validated six sets of primers for Ebola and one set for Zika detection. Our results suggest that the capacity of selective amplification in a conventional thermocycler and in a miniPCR is essentially the same. The use of the miniPCR is intuitive and simple; the user can easily follow the advance of the iterative temperature cycling using a laptop. Despite its compact size, the miniPCR allows a full amplification protocol to be performed in a similar time as in a conventional thermocycler (a difference of only six minutes in a 30-cycle protocol). The mini-PCR thermocycler exhibits the essential attributes of a POC system: (a) the use of small volumes, (b) low capital cost, (c) portability, (d) and a fast, accurate, and selective response. Therefore, this already commercially available and simple nucleic acid amplification system has great potential for use in remote or underprivileged areas, in the case of natural disasters, on the battlefield, or during epidemic emergencies.

In addition, we have documented the effect of using different primers that yield different amplicon sizes, thereby providing a reference resource for primer design for POC applications using the miniPCR. We also provided a detailed account of a strategy for producing Ebola- and ZIKV-related nucleic acids that is free of infection risk in any conventional lab. This is a useful, if not necessarily intuitive, resource that allows personnel to study the virus nucleic acids without the risk of contracting a deadly disease. This straightforward approach will facilitate POC research related to highly infective viruses in underdeveloped regions.

Supporting information

S1 Dataset. Dataset related to Fig 2B and 2C. Evaluation of the amount of miniPCR-amplified DNA (as measured by Nanodrop Spectrometry at 260 nm), and the purity (absorbance ratio at 260/280 nm) of DNA produced by primer sets that produce amplicons of different sizes.
(XLSX)

S2 Dataset. Dataset related to Fig 4B. Average amount of nucleic acid material recovered from the agarose gels.
(XLSX)

S3 Dataset. Dataset related to Fig 4C. Average amount of nucleic acid material recovered, as quantified by SYBR Green qPCR staining and fluorescence measurements in a real time thermocycler.
(XLSX)

S1 Fig. Maps and sequences related to EBOV. A)Vector Map: pCMV Ebola GP. Mammalian Expression Vectors, ampicilin and neomycin resistance, CMV promoter and primers EBOV1, EBOV2, EBOV3, EBOV4, EBOV5 and EBOV6. B) Amino acid sequence alignment from EBOV GenBank 1976–2014 (GP Protein).
(PDF)

S2 Fig. Maps and sequences related to ZIKV. A)Vector map: PUC57 Zika E Clonning vector, ampicilin resistance and primers ZIKV1 y ZIKV2. B) Amino acid sequence alignment from ZIKV GenBank 2013–2016 (E Protein).
(PDF)

Acknowledgments

Author Contributions

Conceptualization: Everardo González-González, Daniel Lira-Serhan, Grissel Trujillo-de Santiago, Mario Moisés Alvarez.

Data curation: Everardo González-González, Jackelin Lizeth Mendoza-Ramos, Sara Cristina Pedroza, Aimé Alexandra Cuellar-Monterrubio.

Formal analysis: Everardo González-González, Jackelin Lizeth Mendoza-Ramos, Grissel Trujillo-de Santiago, Mario Moisés Alvarez.

Funding acquisition: Daniel Lira-Serhan, Grissel Trujillo-de Santiago, Mario Moisés Alvarez.

Investigation: Everardo González-González, Jackelin Lizeth Mendoza-Ramos, Sara Cristina Pedroza, Alan Roberto Márquez-Ipiña.

Methodology: Everardo González-González, Jackelin Lizeth Mendoza-Ramos, Sara Cristina Pedroza, Aimé Alexandra Cuellar-Monterrubio, Alan Roberto Márquez-Ipiña, Mario Moisés Alvarez.

Project administration: Grissel Trujillo-de Santiago, Mario Moisés Alvarez.

Resources: Daniel Lira-Serhan, Mario Moisés Alvarez.

Supervision: Alan Roberto Márquez-Ipiña, Grissel Trujillo-de Santiago, Mario Moisés Alvarez.

Writing – original draft: Jackelin Lizeth Mendoza-Ramos, Mario Moisés Alvarez.

Writing – review & editing: Grissel Trujillo-de Santiago, Mario Moisés Alvarez.

References

1. Yager P, Domingo GJ, Gerdes J. Point-of-Care Diagnostics for Global Health. Annu Rev Biomed Eng. Annual Reviews; 2008; 10: 107–144. https://doi.org/10.1146/annurev.bioeng.10.061807.160524 PMID: 18358075

2. Alvarez MM, Aizenberg J, Analoui M, Andrews AM, Bisker G, Boyden ES, et al. Emerging Trends in Micro- and Nanoscale Technologies in Medicine: From Basic Discoveries to Translation. ACS Nano. American Chemical Society; 2017; 11: 5195–5214. https://doi.org/10.1021/acsnano.7b01493 PMID: 28524668

3. Elizondo-Montemayor L, Alvarez MM, Hern??ndez-Torre M, Ugalde-Casas PA, Lam-Franco L, Busta-mante-Careaga H, et al. Seroprevalence of antibodies to influenza A/H1N1/2009 among transmission risk groups after the second wave in Mexico, by a virus-free ELISA method. Int J Infect Dis. 2011; 15: 0–5. https://doi.org/10.1016/j.ijid.2011.07.002 PMID: 21855383

4. Alvarez MM, López-Pacheco F, Aguilar-Yañez JM, Portillo-Lara R, Mendoza-Ochoa GI, García-Echauri S, et al. Specific Recognition of Influenza A/H1N1/2009 Antibodies in Human Serum: A Simple Virus-Free ELISA Method. Jeyaseelan S, editor. PLoS One. Public Library of Science; 2010; 5: e10176. https://doi.org/10.1371/journal.pone.0010176 PMID: 20418957

5. Kaushik A, Tiwari S, Dev Jayant R, Marty A, Nair M. Towards detection and diagnosis of Ebola virus disease at point-of-care. Biosens Bioelectron. NIH Public Access; 2016; 75: 254–72. https://doi.org/10.1016/j.bios.2015.08.040 PMID: 26319169

6. González-González E, Alvarez MM, Márquez-Ipiña AR, Trujillo-de Santiago G, Rodríguez-Martínez LM, Annabi N, et al. Anti-Ebola therapies based on monoclonal antibodies: current state and challenges ahead. Crit Rev Biotechnol. Taylor & Francis; 2017; 37: 53–68. https://doi.org/10.3109/07388551.2015.1114465 PMID: 26611830

7. Broadhurst MJ, Kelly JD, Miller A, Semper A, Bailey D, Groppelli E, et al. ReEBOV Antigen Rapid Test kit for point-of-care and laboratory-based testing for Ebola virus disease: a field validation study. Lancet. Elsevier; 2015; 386: 867–874. https://doi.org/10.1016/S0140-6736(15)61042-X PMID: 26119838

8. Ferguson NM, Cucunubá ZM, Dorigatti I, Nedjati-Gilani GL, Donnelly CA, Basáñez M-G, et al. EPIDE-MIOLOGY. Countering the Zika epidemic in Latin America. Science. American Association for the Advancement of Science; 2016; 353: 353–4. https://doi.org/10.1126/science.aag0219 PMID: 27417493

9. Mauk MG, Song J, Bau HH, Liu C. Point-of-Care Molecular Test for Zika Infection. Clin Lab Int. NIH Public Access; 2017; 41: 25–27. Available: http://www.ncbi.nlm.nih.gov/pubmed/28819345 PMID: 28819345

10. Meagher RJ, Negrete OA, Van Rompay KK. Engineering Paper-Based Sensors for Zika Virus. Trends Mol Med. Elsevier Current Trends; 2016; 22: 529–530. https://doi.org/10.1016/j.molmed.2016.05.009 PMID: 27255410

11. Jansen van Vuren P, Grobbelaar A, Storm N, Conteh O, Konneh K, Kamara A, et al. Comparative Evaluation of the Diagnostic Performance of the Prototype Cepheid GeneXpert Ebola Assay. J Clin Microbiol. American Society for Microbiology; 2016; 54: 359–67. https://doi.org/10.1128/JCM.02724-15 PMID: 26637383

12. Duchesne L, Lacombe K. Innovative technologies for point-of-care testing of viral hepatitis in low-resource and decentralized settings. J Viral Hepat. John Wiley & Sons, Ltd (10.1111); 2018; 25: 108–117. https://doi.org/10.1111/jvh.12827 PMID: 29134742

13. Pardee K, Green AA, Takahashi MK, Braff D, Lambert G, Lee JW, et al. Rapid, Low-Cost Detection of Zika Virus Using Programmable Biomolecular Components. Cell. Cell Press; 2016; 165: 1255–1266. https://doi.org/10.1016/j.cell.2016.04.059 PMID: 27160350

14. Kaushik A, Tiwari S, Dev Jayant R, Vashist A, Jayant RD, Nikkhah-Moshaie R, et al. Electrochemical Biosensors for Early Stage Zika Diagnostics NanoNeurosurgery View project Sensing systems for point-of-care applications View project Electrochemical Biosensors for Early Stage Zika Diagnostics. 2017; https://doi.org/10.1016/j.tibtech.2016.10.001

15. Yen C-W, de Puig H, Tam JO, Gómez-Márquez J, Bosch I, Hamad-Schifferli K, et al. Multicolored silver nanoparticles for multiplexed disease diagnostics: distinguishing dengue, yellow fever, and Ebola viruses. Lab Chip. The Royal Society of Chemistry; 2015; 15: 1638–1641. https://doi.org/10.1039/c5lc00055f PMID: 25672590

16. Wei T-Y, Cheng C-M. Cell Chemical Biology Synthetic Biology-Based Point-of-Care Diagnostics for Infectious Disease. 2016; https://doi.org/10.1016/j.chembiol.2016.07.016

17. Liao S-C, Peng J, Mauk MG, Awasthi S, Song J, Friedman H, et al. Smart cup: A minimally-instrumented, smartphone-based point-of-care molecular diagnostic device. Sensors Actuators B Chem. Elsevier; 2016; 229: 232–238. https://doi.org/10.1016/J.SNB.2016.01.073 PMID: 26900258

18. Craw P, Balachandran W. Isothermal nucleic acid amplification technologies for point-of-care diagnostics: a critical review. Lab Chip. The Royal Society of Chemistry; 2012; 12: 2469. https://doi.org/10.1039/c2lc40100b PMID: 22592150

19. Hsieh K, Patterson AS, Ferguson BS, Plaxco KW, Soh HT. Rapid, sensitive, and quantitative detection of pathogenic DNA at the point of care through microfluidic electrochemical quantitative loop-mediated isothermal amplification. Angew Chem Int Ed Engl. NIH Public Access; 2012; 51: 4896–900. https://doi.org/10.1002/anie.201109115 PMID: 22488842

20. Pieters M, Daniels J, Rovira A. Comparison of sample types and diagnostic methods for in vivo detection of Mycoplasma hyopneumoniae during early stages of infection. Vet Microbiol. Elsevier; 2017; 203: 103–109. https://doi.org/10.1016/J.VETMIC.2017.02.014 PMID: 28619131

21. Kozel TR, Burnham-Marusich AR. Point-of-Care Testing for Infectious Diseases: Past, Present, and Future. J Clin Microbiol. American Society for Microbiology; 2017; 55: 2313–2320. https://doi.org/10.1128/JCM.00476-17 PMID: 28539345

22. Su W, Gao X, Jiang L, Qin J. Microfluidic platform towards point-of-care diagnostics in infectious diseases. J Chromatogr A. Elsevier; 2015; 1377: 13–26. https://doi.org/10.1016/j.chroma.2014.12.041 PMID: 25544727

23. Drancourt M, Michel-Lepage A, Boyer S, Raoult D. The Point-of-Care Laboratory in Clinical Microbiology. Clin Microbiol Rev. American Society for Microbiology; 2016; 29: 429–47. https://doi.org/10.1128/CMR.00090-15 PMID: 27029593

24. Kersting S, Rausch V, Bier FF, Von Nickisch-Rosenegk M. Multiplex isothermal solid-phase recombinase polymerase amplification for the specific and fast DNA-based detection of three bacterial pathogens. 2014; Available: https://link.springer.com/content/pdf/10.1007/s00604-014-1198-5.pdf PMID: 25253912

25. Jangam SR, Agarwal AK, Sur K, Kelso DM. A point-of-care PCR test for HIV-1 detection in resource-limitedsettings. Biosens Bioelectron. Elsevier; 2013; 42: 69–75. https://doi.org/10.1016/j.bios.2012.10.024 PMID: 23202333

26. Qiu X, Ge S, Gao P, Li K, Yang S, Zhang S, et al. A smartphone-based point-of-care diagnosis of H1N1 with microfluidic convection PCR. Microsyst Technol. Springer Berlin Heidelberg; 2017; 23: 2951–2956. https://doi.org/10.1007/s00542-016-2979-z

27. Marx V. PCR heads into the field. Nat Methods. 2015; 12: 393–397. https://doi.org/10.1038/nmeth.3369 PMID: 25924072

28. Kwon H-S, Park H-C, Lee K, An S, Oh Y-L, Ahn E-R, et al. Performance of MiniPCR ™ mini8, a portable thermal cycler. Anal Sci Technol. The Korean Society of Analytical Science; 2016; 29: 79–84. https://doi.org/10.5806/AST.2016.29.2.79

29. Guevara EE, Frankel DC, Ranaivonasy J, Richard AF, Ratsirarson J, Lawler RR, et al. A simple, economical protocol for DNA extraction and amplification where there is no lab. Conserv Genet Resour. Springer Netherlands; 2018; 10: 119–125. https://doi.org/10.1007/s12686-017-0758-5

30. Pomerantz A, Peñafiel N, Arteaga A, Bustamante L, Pichardo F, Coloma LA, et al. Real-time DNA barcoding in a rainforest using nanopore sequencing: opportunities for rapid biodiversity assessments and local capacity building. Gigascience. Oxford University Press; 2018; 7. https://doi.org/10.1093/gigascience/giy033 PMID: 29617771

31. Boguraev A-S, Christensen HC, Bonneau AR, Pezza JA, Nichols NM, Giraldez AJ, et al. Successful amplification of DNA aboard the International Space Station. npj Microgravity. 2017; 3. https://doi.org/10.1038/s41526-017-0033-9 PMID: 29167819

32. Montague TG, Almansoori A, Gleason EJ, Copeland DS, Foley K, Kraves S, et al. Gene expression studies using a miniaturized thermal cycler system on board the International Space Station. Reddy S V., editor. PLoS One. Public Library of Science; 2018; 13: e0205852. https://doi.org/10.1371/journal.pone.0205852 PMID: 30379894

33. Zaky WI, Tomaino FR, Pilotte N, Laney SJ, Williams SA. Backpack PCR: A point-of-collection diagnostic platform for the rapid detection of Brugia parasites in mosquitoes. McCarthy JS, editor. PLoS Negl Trop Dis. Public Library of Science; 2018; 12: e0006962. https://doi.org/10.1371/journal.pntd.0006962 PMID: 30462640

34. Chin CD, Linder V, Sia SK. Commercialization of microfluidic point-of-care diagnostic devices{. https://doi.org/10.1039/c2lc21204h

35. Kuhn JH. Guide to the Correct Use of Filoviral Nomenclature. Springer, Cham; 2017. pp. 447–460. https://doi.org/10.1007/82_2017_7

36. Malone RW, Homan J, Callahan M V., Glasspool-Malone J, Damodaran L, Schneider ADB, et al. Zika Virus: Medical Countermeasure Development Challenges. Kading RC, editor. PLoS Negl Trop Dis. Public Library of Science; 2016; 10: e0004530. https://doi.org/10.1371/journal.pntd.0004530 PMID: 26934531

37. Holmes EC, Dudas G, Rambaut A, Andersen KG. The evolution of Ebola virus: Insights from the 2013–2016 epidemic. Nature. Nature Publishing Group; 2016; 538: 193–200. https://doi.org/10.1038/nature19790 PMID: 27734858

38. Smither SJ, Eastaugh L, Ngugi S, O'Brien L, Phelps A, Steward J, et al. Ebola Virus Makona Shows Reduced Lethality in an Immune-deficient Mouse Model. J Infect Dis. Oxford University Press; 2016; 214: S268–S274. https://doi.org/10.1093/infdis/jiw145 PMID: 27471321

39. Broude NE, Zhang L, Woodward K, Englert D, Cantor CR. Multiplex allele-specific target amplification based on PCR suppression. Proc Natl Acad Sci U S A. National Academy of Sciences; 2001; 98: 206–11. https://doi.org/10.1073/pnas.98.1.206 PMID: 11136256

40. Edwards MC, Gibbs RA. ll|llllManual Supplement Multiplex PCR: Advantages, Development, and Applications. Available: https://genome.cshlp.org/content/3/4/S65.full.pdf

41. Debode F, Marien A, Janssen É, Bragard C, Berben G. B A S E The influence of amplicon length on real-time PCR results [Internet]. Biotechnol. Agron. Soc. Environ. 2017. Available: http://www.pressesagro.be/base/text/v21n1/3.pdf